A APPENDIX

A.1 One-step Denoising Experiments

We have included additional figures for our one-step denoiser experiments. Figures 5 and 6 show the one step denoiser performance of the various methods at the measurement noise level and a lower test noise level for the AFHQ and NBU datasets respectively. We observe that our method performs better at denoising below the measurement noise level compared to other self-supervised denoising techniques.

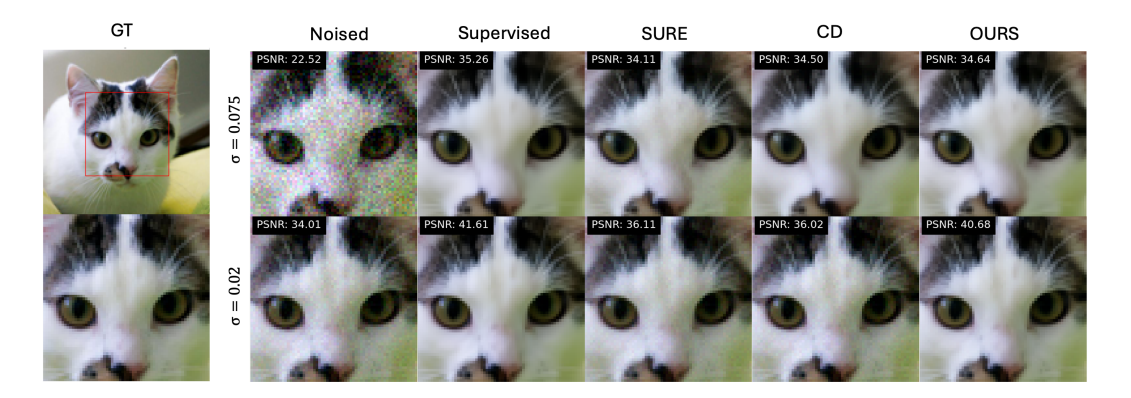


Figure 5: Example restorations of various denoisers on AFHQ dataset at test noise levels $\sigma_t = 0.075$ (top) and $\sigma_t = 0.02$ (bottom). All models, except for supervised were trained on only noisy data with $\sigma_n = 0.075$.

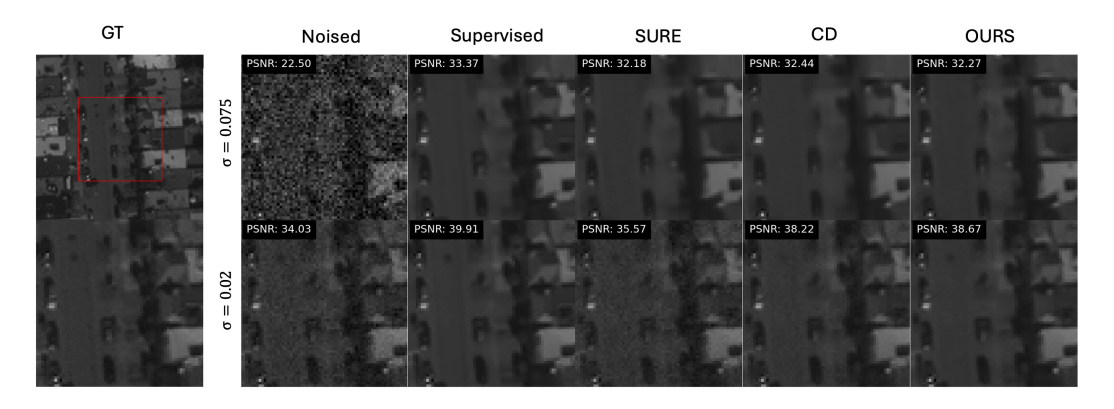


Figure 6: Example restorations of various denoisers on NBU dataset at test noise levels $\sigma_t = 0.075$ (top) and $\sigma_t = 0.02$ (bottom). All models, except for supervised were trained on only noisy data with $\sigma_n = 0.075$.

A.2 DIFFUSION SAMPLING

Additional figures have been provided for diffusion sampling experiments on the AFHQ and NBU datasets. Figures 7 and 8 show example diffusion samples for supervised and self-supervised approaches discussed in the paper on AFHQ and NBU respectively. Figure 9 shows diffusion samples for different training + inference noise levels with accompanying radial spectrum plots in Figure 10. Here we see that while one-step supervised and self-supervised MMSE denoisers tend to reduce high frequency features, our method retains higher frequencies lending to our method providing better perceptual images.

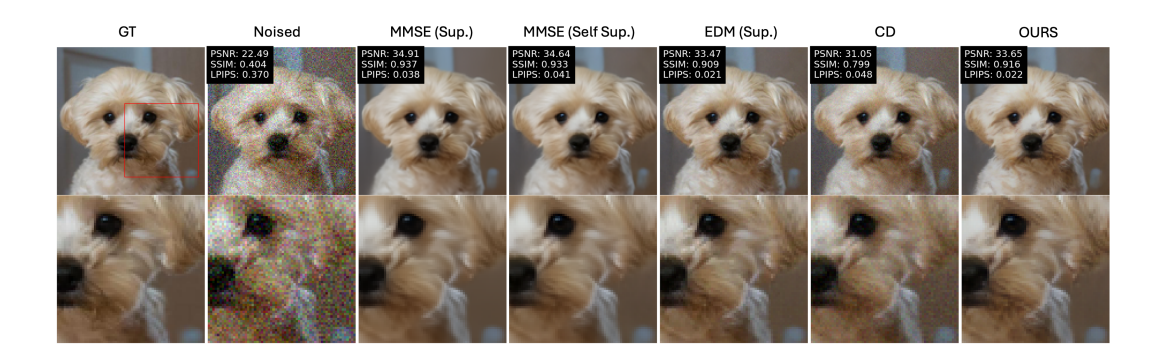


Figure 7: Example of various denoisers using diffusion sampling (except MMSE(Self Sup.) and MMSE(Sup.) columns) on AFHQ dataset with training and test noise level $\sigma_n = \sigma_t = 0.075$.

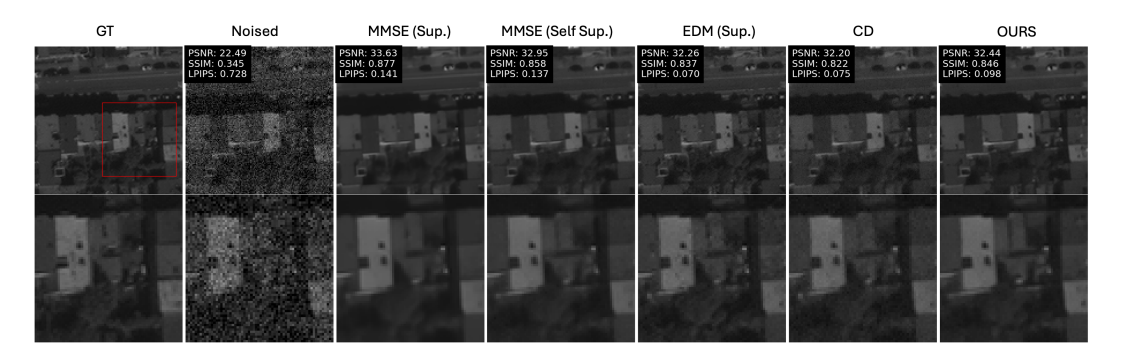


Figure 8: Example of various denoisers using diffusion sampling (except MMSE(Self Sup.) and MMSE(Sup.) columns) on NBU dataset with training and test noise level $\sigma_n = \sigma_t = 0.075$.

A.3 EXTENSION TO LINEAR INVERSE PROBLEMS

We provide example reconstructions for the inpainting and demosaicing tasks in Figures [1] and [12] respectively.

A.4 INFERENCE PROCEDURE

For diffusion sampling in our experiments we use a slightly modified version of the samplers proposed in Karras et al. (2022) by conducting sampling in measurement space. We show the inference procedure in Algorithm 1.

Algorithm 1 Equivariant Sampling Inference

```
Require: D_{\theta}(\cdot, \sigma), \{\sigma_K = \sigma_n, \dots, \sigma_1 = \sigma_{\min}\}, y
  1: \mathbf{y}_{\text{next}} = \mathbf{y}
2: for i \in \{K, \dots, 1\} do
  3:
                      \mathbf{y}_{cur} = \mathbf{y}_{next}
                      \hat{\mathbf{x}} = \left(\mathbf{x}_{\text{cur}} - \mathbf{D}_{\boldsymbol{\theta}}(\mathbf{A}^{\top}\mathbf{y}_{\text{cur}}, \sigma_i)\right) / \sigma_i
  4:
  5:
                      \mathbf{y}_{\text{next}} = \mathbf{y}_{\text{cur}} + 2(\sigma_{i+1} - \sigma_i)\mathbf{A}\hat{\mathbf{x}}
                      \eta \sim \mathcal{N}(\mathbf{0}, \mathbf{I})
  6:
  7:
                      \mathbf{y}_{\text{next}} = \mathbf{y}_{\text{next}} + \sqrt{2(\sigma_{i+1} - \sigma_i)\sigma_i}\,\boldsymbol{\eta}
  8:
                      if i > 1 then
  9:
                                 \hat{\mathbf{x}}' = (\mathbf{x}_{\text{next}} - \mathbf{D}_{\boldsymbol{\theta}}(\mathbf{A}^{\top}\mathbf{y}_{\text{next}}, \sigma_{i+1}))/\sigma_{i+1}
10:
                                 \mathbf{y}_{\text{next}} = \mathbf{y}_{\text{cur}} + \frac{1}{2}(\sigma_{i+1} - \sigma_i)\mathbf{A}(\hat{\mathbf{x}} + \hat{\mathbf{x}}')
11: return \hat{\mathbf{x}}
```



Figure 9: Example reconstructions for different training + inference noise levels on AFHQ.

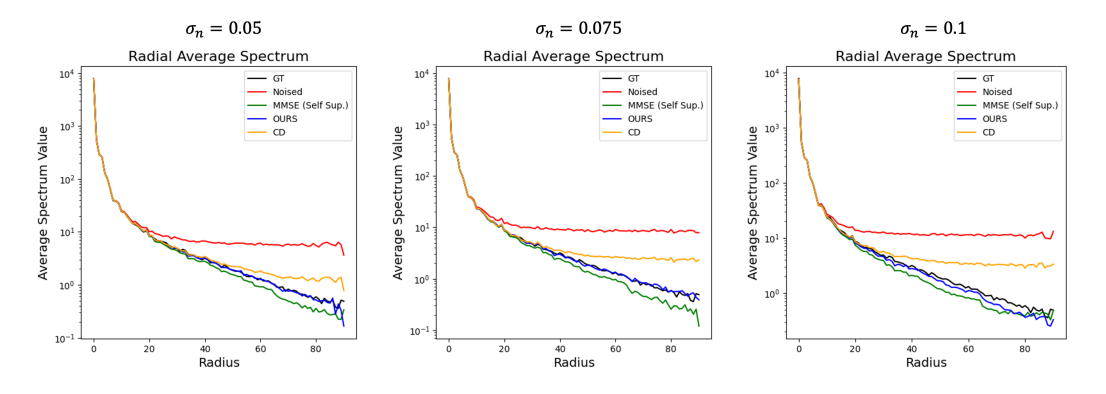


Figure 10: Radial Spectrum of images in Figure 9

A.5 PATCH NORMS

To investigate the assumption that many real image distributions are approximately scale-invariant we plot the histogram of patch-wise norms for several image distributions using various patch sizes in Figure [13]. We see that, in fact, we have a spread in energy within each dataset which implies we may be observing a dataset that exhibits weak invariance.

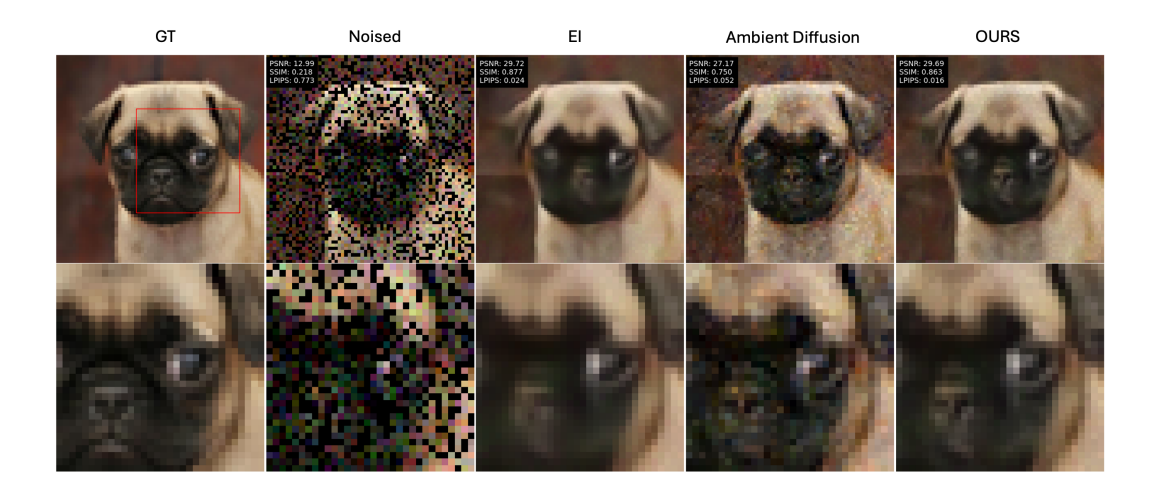


Figure 11: AFHQ inpainting example where the models are all trained in a self-supervised fashion.

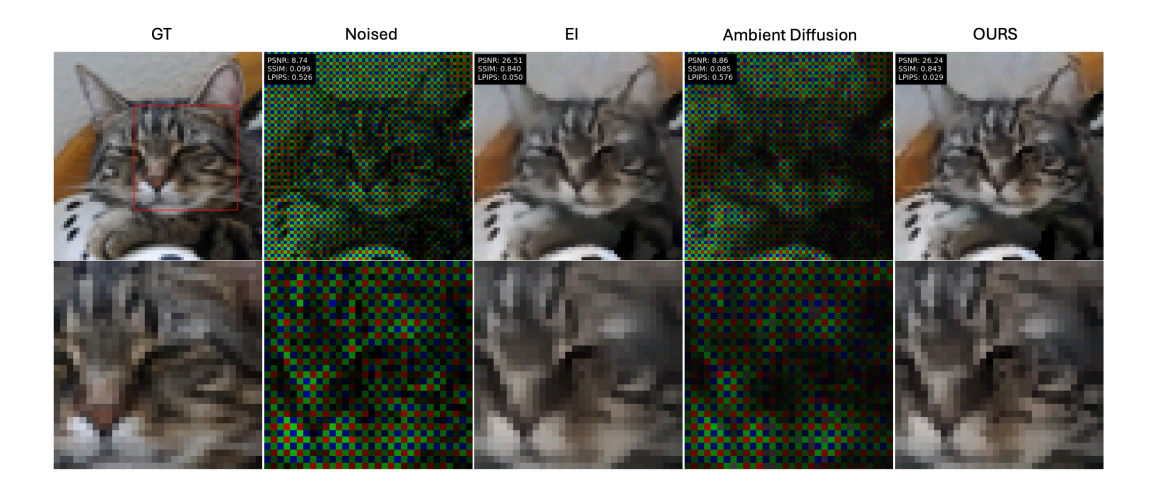


Figure 12: AFHQ demosaic example where the models are all trained in a self-supervised fashion.

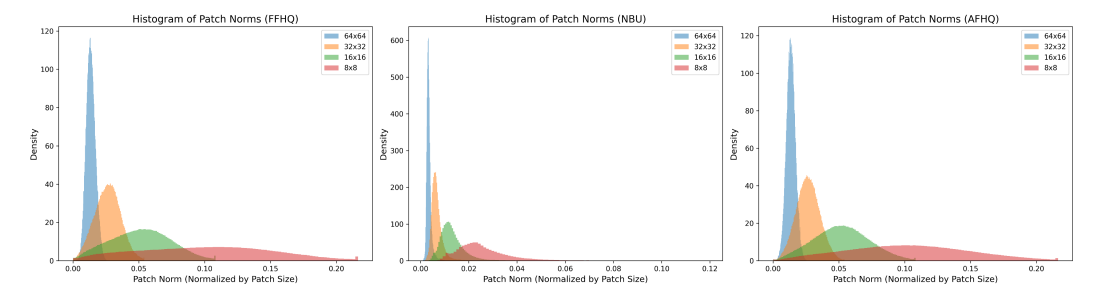


Figure 13: Histogram of image patches for each image distribution.